Research Square

Preprints are preliminary reports that have not undergone peer review.
They should not be considered conclusive, used to inform clinical practice,
or referenced by the media as validated information.

Field deployable viral genomic surveillance using panviral integrated indexed primers

Anna S. Fomsgaard
Institut Pasteur du Cambodge, Phnom Penh
Irene K. Meki
International Atomic Energy Agency
Heidi Auerswald
Istituto Zooprofilattico Sperimentale dell'Abruzzo e del Molise Giuseppe Caporale
Paul F. Horwood
James Cook University
Roslyn I. Hickson
James Cook University, Cairns and Townsville
Brian Merritt
Johns Hopkins Applied Physics Laboratory
Peter Thielen
Johns Hopkins Applied Physics Laboratory
Charles E. Lamien
International Atomic Energy Agency
Erik A. Karlsson
ekarlsson@pasteur-kh.org

Institut Pasteur du Cambodge, Phnom Penh

Article

Keywords: genomic surveillance, nanopore sequencing, zoonotic viruses, field-deployable diagnostics, panviral primers, One Health, outbreak detection, environmental surveillance, live bird markets, emerging infectious diseases, decentralized diagnostics, influenza, coronavirus, rabies, arbovirus

Posted Date: October 30th, 2026

DOI: https://doi.org/10.21203/rs.3.rs-11508835/v1

License: This work is licensed under a Creative Commons Attribution 4.0 International License. Read Full License

Additional Declarations: No competing interests reported.

Abstract

Rapid viral identification near the point of emergence could support outbreak investigation where sequencing infrastructure is limited. The Panviral integrated indexed Primer (PiiP) assay combines broadly reactive viral primers with integrated Oxford Nanopore indices and offline analysis. The workflow was evaluated using human, animal, and environmental samples from Cambodia and deployed with a portable laboratory at a live bird market under tropical conditions. Laboratory evaluation demonstrated detection across diverse sample matrices, although sensitivity varied by viral target and influenza subtype assignment was limited. During field deployment, environmental samples, including air samples, were processed on site, with initial viral read characterization available within 6.5 hours of sample receipt. The workflow reduces library preparation steps and enables same day viral screening outside centralized laboratories. These findings support further evaluation of PiiP for decentralized genomic surveillance, with confirmatory analysis required for uncertain taxonomic assignments.

Introduction

Emerging and re-emerging pathogens threaten human, livestock, and wildlife health. Early detection can influence whether an outbreak is contained or escalates, with substantial human, animal, and economic consequences[1–4]. Rapid characterization of causative agents supports appropriate response measures[5]. Detection near the time and place of emergence is particularly relevant in Southeast Asia, where high biodiversity, intensive human–animal interfaces in traditional markets and agriculture, rapid land-use change, and tropical climates contribute to zoonotic disease emergence[6,7]. Cambodia exemplifies these conditions through avian influenza circulation in live bird markets[8], bat coronaviruses including SARS-CoV-2-related lineages[9], endemic dog-mediated rabies[10], and the urban expansion of *Aedes* mosquitoes[11]. However, limited diagnostic infrastructure outside the capital creates a geographic mismatch between surveillance needs and laboratory access.

Pathogen detection approaches like PCR, qPCR, LAMP tests, antigen tests, and serology provide sensitive, rapid, and cost-effective testing for recognized pathogens, but their use depends on pre-hypothesized targets. This requirement can limit or prolong investigations of unexplained disease clusters or emerging pathogens. Targeted and untargeted sequencing support pathogen detection and characterization, although each has limitations. Amplicon sequencing can be highly sensitive, but primers may require redesign as viral genomes evolve. Untargeted metagenomic sequencing offers broader detection, yet recovering viral sequences from complex backgrounds remains challenging[12]. Hybridization-based capture sequencing enriches known pathogens and can sometimes recover genetically distant material[13]. However, shared with abovementioned approaches, it can be labor-intensive and costly, involve multiple processing steps, and require substantial bioinformatics expertise[14]. While these approaches remain essential, complementary methods that combine broad viral targeting with simpler preparation and rapid analysis could improve the accessibility and practicality of sequencing for surveillance.

Panviral primers target conserved regions to amplify known and genetically divergent viruses, reducing reliance on untargeted metagenomic sequencing[15,16]. This approach can support outbreak investigations by targeting conserved regions within viral families or genera while retaining sequence variation useful for characterization[17–20]. The Panviral integrated indexed Primer (PiiP) assay targets *Alphainfluenzavirus*, coronaviruses, *Orthoflavivirus*, and *Lyssavirus*. Oxford Nanopore indices integrated into the forward primer enable reverse transcription, amplification, and indexing in a single reaction[21,22]. This strategy removes individual end-preparation and barcode ligation steps and reduces bead-based purification, hands-on processing, and workflow complexity.

Rapid data analysis remains a barrier to field sequencing. Platforms such as CZID, Genome Detective, and Galaxy workflows have made pathogen sequence analysis more accessible[23–25], but deployments that require internet access, cloud computing, or transfer of completed datasets can be difficult to use in remote settings. Waiting for sequencing to finish also delays interpretation. An open-source pipeline deployed offline on a laptop (https://github.com/jhuapl-bio/mytax) was therefore used to analyze Oxford Nanopore reads as they were generated[26]. Automated taxonomic classification and visualization can reduce the expertise and data transfer required for initial viral identification, although assignment accuracy depends on the target sequence and reference database.

This study developed and evaluated a workflow combining broadly reactive indexed primers, real-time Nanopore sequencing, and offline analysis for viral screening outside centralized laboratories. Performance was assessed using spiked matrices and human, animal, and environmental samples from Cambodia, followed by deployment of the workflow in an assembled portable laboratory at a live bird market. The evaluation examined detection across viral targets and sample types, taxonomic assignment, and the feasibility of same day identification under field conditions. The workflow targets selected viral groups rather than providing unrestricted pathogen discovery, and species or subtype assignments require interpretation within the resolution of the amplified region.

Results

Detection thresholds in spiked matrices

The analytical sensitivity of the PiiP assay and the potential effects of inhibitory sample matrices were assessed by spiking virus-negative specimens with cultured stocks of the targeted viral genera.

Influenza A H5N1 in chicken swabs

To evaluate PiiP assay performance under realistic surveillance conditions, chicken throat swabs were used as the spiking matrix. The PiiP assay detected *Alphainfluenzavirus* across Cq values 16.2–36.9 (10^2–10^7 dilution) with 100% sensitivity and specificity. Reads were predominantly assigned to H5N1 up to Cq ≤ 33.1 (Fig. 2a; Supplementary Data 1, worksheet Table S4-A). Automated real-time analysis occasionally misclassified reads belonging to subtype H7N9 and H9N2; however, the number of reads assigned to H5N1 remained significantly higher than those assigned to other subtypes (repeated-measures one-way ANOVA, $p = 0.0277$). MyTax2 additionally assigned reads to orthobunyavirus spp. in three dilutions (10^4, 10^6, and 10^7). Manual inspection in Geneious Prime demonstrated that they represented short terminal alignments to orthobunyavirus reference genomes rather than true orthobunyavirus-derived sequences. The majority of reads mapped to Influenza A virus (A/chicken/Guangdong/1/2005(H5N1)) segment 7 matrix protein genes (M1/M2; accession EU874901), with the expected *Alphainfluenzavirus* PiiP primers flanking the approximately 166 bp amplicon.

Coronavirus in homogenized bat gut

Serial dilutions of SARS-CoV-2 were spiked into homogenized bat gut tissue to assess assay performance in a wildlife-derived matrix. The PiiP assay detected the *Betacoronavirus* genus and identified SARS-CoV-2 across Cq values 21.6–34.2 (10^2-10^6 dilution), with 83.3% sensitivity and 100% specificity (Fig. 2b; Supplementary Data 1, worksheet Table S4-A). No detection was observed at the highest dilution (10^7; Cq 36.1). Low numbers of

Alphainfluenzavirus reads were identified in the samples during MyTax2 analysis; however, all read counts remained below the empirically defined threshold established from negative controls, and were therefore classified as negative for *Alphainfluenzavirus*.

Orthoflavivirus in homogenized mosquitoes

Serial dilutions of dengue virus serotype 1 (DENV-1) were spiked into homogenized *Ae. albopictus* to assess assay performance in an arthropod-derived matrix. The PiiP assay detected *Orthoflavivirus* across Cq values 24.5–39.6, corresponding to 10–10^6 dilutions, with 100% sensitivity and specificity. The 10^7 dilution was excluded, as it tested negative by qPCR for DENV-1. Correct DENV-1 serotyping was achieved at Cq ≤ 32.0 (Fig. 2c; Supplementary Data 1, worksheet Table S4-A). Amplification band intensity did not decrease with increasing dilution, and an *Orthoflavivirus* amplicon-sized band was observed in the DENV-1 negative mosquito pool control, while the negative water control remained negative. Sequencing revealed insect-specific flaviviruses most closely related to Mosquito flavivirus isolate MOF_Aa-188_TI2016 (Accession no.: MN566101) and *Aedes* flavivirus strain HB_C9_18-7-HZ-Aea-B-4-JG-1 (Accession no.: MW246700) (Supplementary Table 1). Small numbers of influenza A reads were detected in sequenced samples. All read counts, except for one dilution step (10^6), remained below the empirically defined threshold, consistent with negative classifications for influenza A.

Lyssavirus in homogenized dog brain

Rabies virus (RABV) infection in dogs is typically confirmed post-mortem by testing brain tissue. Serial dilutions of RABV were spiked into homogenized dog brain tissue to assess assay performance. The PiiP assay detected the *Lyssavirus* genus and correctly identified RABV across Cq values 19.8–30.0 (Fig. 2d; Supplementary Data 1, worksheet Table S4-A). No amplification was observed at higher dilutions corresponding to Cq 33.5 and 35.6, resulting in an overall sensitivity of 66.7% and specificity of 100%. Surveillance data from Institut Pasteur du Cambodge indicate that post-mortem Cq values for RABV in dog brains typically cluster around Cq 20, consistent with these findings. *Alphainfluenzavirus* reads were detected in samples, but all counts remained below the empirically defined threshold, resulting in negative classifications for *Alphainfluenzavirus*.

Influenza A/H5N1 in environmental samples

Environmental sampling presents unique challenges compared to host-derived specimens, yet it is critical for real-world pathogen surveillance. Viruses such as avian influenza can be shed into the environment and remain infectious, posing risks to animals and humans. Serial dilutions of H5N1 were spiked into poultry wash water to assess assay performance in an environmental matrix. The PiiP assay detected *Alphainfluenzavirus* and predominantly assigned reads to H5N1 across Cq values 17.1–36.2, with 100% sensitivity and specificity (Fig. 2e; Supplementary Data 1, worksheet Table S4-A). Minor read misassignments to H7N9 and H9N2 were observed, but H5N1 remained significantly more frequent (repeated-measures one-way ANOVA, $p = 0.007$). These results indicate that the assay can detect avian influenza viruses in environmental samples, supporting its application for non-invasive surveillance in live bird markets.

Fourplex assay performance

Following individual evaluation of each viral target, PiiP assays were combined in a fourplex format to assess assay performance for broad-spectrum surveillance. Samples of known virus content produced expected amplicon sizes for each sample (Fig. 3a). Genus-level classification accuracy remained high, with nearly all reads assigned correctly. At the species/subtype level, accurate assignments were obtained for SARS-CoV-2 (99.68%), DENV-1 (96.81%), DENV-2 (94.67%), Japanese encephalitis virus (JEV) (99.73%), Zika virus (ZIKV) (99.29%), and RABV (95.87%) (Fig. 3b; Supplementary Data 1, worksheet Table S4-B). For Alphainfluenzaviruses, subtype resolution varied. H1N1 and H3N2 were identified with high accuracy (88.26% and 95.64%, respectively), whereas H5N1, H7N7, and H9N2 showed misclassification (Fig. 3b; Supplementary Data 1, worksheet Table S4-B). H7N7 in particular yielded no correctly assigned reads. DENV-1 had 489 reads (1.6%) assigned to cell-fusing agent virus and DENV-2 had 1068 reads (3.3%) assigned to Cacipacore virus (Supplementary Data 1, worksheet Table S4-B). Multiplexing capacity was further assessed using artificial viral mixtures of H5N1, SARS-CoV-2, DENV-1, and RABV. All combinations were detected by both gel electrophoresis (Fig. 3c) and sequencing using Geneious Prime data analysis (Fig. 3d; Supplementary Data 1, worksheet Table S4-C). In mixtures containing three or four targets, read distribution varied between viruses, with SARS-CoV-2 consistently producing fewer read counts than other targets (Fig. 3d).

Detection in environmental animal and human samples

The PiiP assay was evaluated using 73 samples of environmental, animal, and human origin collected through ongoing and previous pathogen surveillance efforts in Cambodia (Fig. 4a,c).

Alphainfluenzaviruses

Nineteen samples from live bird markets and eleven human clinical samples were tested. The qPCR-confirmed positive samples had Cq values ranging from 18.1–40.2. The predominant PiiP read assignments agreed with qPCR subtyping results up to Cq 33.3 (Supplementary Data 1, worksheet Table S4-D). In two air samples and three throat swabs with Cq 33.3–40.2, virus was not detected. Two biological negative controls (air sample, duck throat swab) were correctly classified as negative. Despite occasional read misassignments to other influenza subtypes, the highest read count consistently matched the qPCR subtype except for one qPCR subtyped H5N1/H9NX sample misclassified as H1N1. Human clinical samples had Cq values of 15.2–33.8. All were detected, with reads assigned to H1N1 or H3N2 in agreement with the known sample subtype, without misassignments (Supplementary Data 1, worksheet Table S4-D).

Coronaviruses

Eleven clinical human samples and ten bat rectal swabs were processed. All ten SARS-CoV-2 human samples (Cq 21.0–36.7) were correctly classified as SARS-CoV-2. Among the ten bat samples, two contained Betacoronaviruses (Cq 29.0 and 31.4). Automated analysis with the MyTax2 module detected one, whereas Geneious Prime analysis identified betacoronavirus reads in both, with alignments to bat coronavirus clone BANAL-236 (Accession no.: PP856574) and a SARS-CoV-2 isolate (Accession no.: OR086674), respectively.

Eight bat samples contained Alphacoronaviruses. Automated analysis using the Kraken2 RefSeq viral database, which contains 28 previously established reference sequences, failed to identify them, but Geneious Prime analysis revealed alignments to Bat alphacoronaviruses for four of the samples: PH201 isolate AlphaCoV PH201 (Accession no.: OM219639), MAG: Bat HKU2-like alphacoronavirus LS1 isolate BtCoV/RtLS01 (Accession no.:

OQ709196), Bat coronavirus HKU2 strain HKU2/HK/33/2006 (Accession no.: EF203067), and Bat Coronavirus RaGD19 isolate BtRa-AlphaCoV/GD2019-Q210 (Accession no.: OQ175201) (Supplementary Table 2). In the remaining four samples, two yielded a small number of sequencing reads aligning to SARS-CoV-2 (Accession no.: OV192362), while two showed no coronavirus reads (Supplementary Table 2).

Orthoflaviviruses

Eleven laboratory-reared mosquitoes were processed, including nine infected with DENV-1 (Cq 20.9–41.8). The PiiP assay consistently detected DENV-1 with correct genus- and serotype-level assignment up to Cq 33.9. The insect-specific Orthoflaviviruses were also detected in a non-infected *Ae. albopictus* mosquito, and the cell-fusing agent virus in an *Ae. aegypti* mosquito (Supplementary Data 1, worksheet Table S4-D). The cell-fusing agent virus is known to infect *Ae.* aegypti among others, and belongs to the genus *Orthoflavivirus*, previously named Flavivirus.

Lyssaviruses

Ten dog brain swab samples and one RABV-negative macaque brain control were analyzed. Positive samples had Cq values 16.2–20.1. RABV was detected with high coverage depth in all RABV positive samples (Supplementary Data 1, worksheet Table S4-D). The negative control was confirmed negative. In one sample, the Kraken2 RefSeq viral database assigned a minority of reads to Lagos bat virus, but Geneious Prime re-analysis confirmed exclusive alignment to RABV (Accession no.: OP515340).

Field deployment test-of-concept

The PiiP assay was deployed outdoors in Phnom Penh, Cambodia, using the portable field laboratory. Eight environmental samples from the Orussey live bird market were collected and immediately processed with a negative H_2O control on site (Fig. 4b). Parallel testing of samples back at the reference laboratory with subtyping RT-qPCR assays detected influenza A H9 and H5 in all samples (Supplementary Data 1, worksheet Table S4-E), with lower Cq values for H9 (median 28.9, IQR 4.5) compared to H5 (median 33.1, IQR 4.5). One wash water sample (Cq 36.6) and one air sample (Cq 37.3) were positive for H7. The full PiiP assay was completed within 6.5 hours from sample receipt to first viral read characterization and visualization in the MyTax2 module. The PiiP analysis assigned reads to H3, H7, and H9 subtypes within 5 minutes of sequencing, followed shortly by bird *Gammacoronavirus*. Influenza A virus (A/Hong Kong/1073/99(H9N2)) consistently had more reads classified than any other subtype. Reads were also classified as H7N9, H3N2, and H1N1. RT-qPCR detected IBV in all samples (median Cq 20.6, IQR 2.9). PiiP analysis assigned reads to IBV in all but one drinking water sample (Cq 22.1), which yielded no IBV-assigned reads but was classified as avian coronavirus.

Discussion

The PiiP assay enabled same day viral screening with a portable laboratory deployed at a live bird market in Cambodia. Integrating indexed panviral primers, simplified library preparation, and offline analysis reduced processing steps and supported initial read characterization within 6.5 hours of sample receipt. Laboratory evaluation demonstrated detection across human, animal, and environmental matrices, while field deployment established feasibility for environmental samples under tropical conditions. These findings support further evaluation at human–animal interfaces where access to centralized sequencing is limited. The study demonstrates technical and operational feasibility; effects on outbreak response or transmission were not measured.

The viral groups targeted by the PiiP assay (*Alphainfluenzavirus*, coronaviruses, *Orthoflavivirus*, and *Lyssavirus)* include zoonotic pathogens with distinct host ranges and outbreak dynamics that typify the zoonotic emergence landscape in Southeast Asia. Alphainfluenzaviruses such as avian influenza circulate widely in live bird markets where virus particles shed into the environment pose infection risks for both animals and humans[8]. The PiiP assay's ability to detect viral RNA from both direct and environmental samples (e.g. air samples) demonstrates its suitability for non-invasive surveillance, complementing other proposed surveillance approaches[27]. Coronaviruses detected in regional bat populations, including SARS-CoV-2-related lineages in Cambodia, support continued genomic surveillance and reservoir monitoring[9,28,29]. Orthoflaviviruses, often transmitted by *Aedes* mosquitoes, are increasingly found in urban areas such as Phnom Penh[11], with global examples like Brazil in 2015 showing how rapidly flaviviruses can spread and impact public health[30]. The PiiP assay's detection of Orthoflaviviruses and background insect-specific viruses highlights its potential value for arbovirus surveillance and entomological investigations in hotspot areas like Cambodia. Rabies also remains endemic in the region, with dogs as the main reservoir and source of human infection[10]. Reliable molecular detection of RABV directly from dog brain samples supports further evaluation for use in rural diagnostic settings. Beyond rabies, field-deployable detection of lyssaviruses e.g. in bats may support rapid investigation of wildlife mortality events, wildlife-human exposure incidents, and help identify locations where lyssaviruses are circulating, guiding subsequent sampling and confirmatory testing. Together, these targets provide a targeted One Health surveillance panel, encompassing respiratory, vector-borne, and direct-contact transmission routes across avian, mammalian, and arthropod reservoirs.

In the spiking experiments, reported genus-level specificity was 100%, although one influenza A false-positive classification occurred in the flavivirus experiment. Detection decreased at low viral loads for betacoronaviruses and lyssaviruses. IPC surveillance data indicate that post-mortem RABV Cq values in dog brain typically cluster around 20, within the range detected here. Coronavirus performance varied across samples. Artificial viral mixtures consistently yielded fewer SARS-CoV-2 reads than other targets, suggesting possible primer competition, although this mechanism was not established. Multiplex interpretation must therefore account for differences in amplification efficiency, particularly for highly degenerate coronavirus primers. SARS-CoV-2 was detected in a human sample at Cq 36.7, whereas automated analysis did not identify alphacoronaviruses in the bat samples. No in-house alphacoronavirus qPCR assay was available, so low viral loads remain a possible explanation that could not be assessed directly. Expanding primer pools may broaden detection but can increase competition and reduce sensitivity for individual targets. Primer concentrations were optimized and evaluated across diverse viruses and matrices, but periodic revision may be needed as viral lineages evolve[31]. Reference coverage also limited automated classification. Three of the four alphacoronaviruses identified by Geneious Prime (OM219639, OQ709196, and OQ175201) were absent from the Kraken2 RefSeq viral database. However, Bat coronavirus HKU2 strain HKU2/HK/33/2006 was represented, and two samples yielded no coronavirus reads even during Geneious Prime analysis. Database incompleteness therefore explains only part of the detection failure. Minor off-target assignments also occurred in single-virus flavivirus controls. Shared k-mers in conserved NS5 regions could contribute to these assignments, but this explanation remains unconfirmed. Rapid k-mer classification depends on reference coverage and taxonomic resolution. These results support complementary rapid field classification and subsequent sequence review, together with database curation, inclusion of regional viral lineages, and data sharing between sequencing sites.

Influenza subtype assignment was limited because the PiiP primers target the conserved matrix gene. Although the subtype identified by targeted qPCR generally received the most assigned reads, high sequence identity among

co-circulating variants limits subtype differentiation from this region. PiiP results should therefore be interpreted primarily as influenza A detection, with provisional subtype-associated read assignments requiring confirmation. In an outbreak investigation, initial detection could support response decisions while samples undergo reference laboratory testing and whole-genome sequencing[22].

Single-end integrated Oxford Nanopore indexing simplified the workflow and reduced indexed primer costs. Although dual-end indexing can improve demultiplexing, it would increase the costs due to oligo length, and ambiguous reads in the single-end approach remained unclassified rather than being assigned to a sample. As part of the simplified field-deployable workflow, individual sample quantification and normalization were omitted, while the pooled library was quantified and normalized. Read counts consequently reflect differences in viral load, amplification efficiency, and library input and should not be interpreted as quantitative measures of target abundance. This variation requires consideration even when the intended application is screening. Reuse of washed R.10v flow cells previously used for influenza sequencing reduced consumable costs but introduced residual influenza A reads in several barcodes, including negative controls. Incomplete removal of the previous library is a possible explanation; Oxford Nanopore reports potential carryover of 0.1% between washes[32]. A run-specific threshold of three times the corresponding negative-control read count was applied to reduce false-positive classifications[33]. A single influenza A false-positive classification remained in the flavivirus spiking experiment, illustrating the limitations of this empirical threshold. Reusing flow cells may increase throughput per unit cost, but its suitability depends on the consequences of false-positive and false-negative classifications. Carryover-derived reads required little additional analytical effort in this study, but they still required explicit interpretation. More distinct indexing schemes or unused flow cells for critical investigations could be evaluated to reduce carryover and barcode assignment concerns.

The PiiP assay was designed to simplify sensitive pathogen surveillance for deployment in outbreak situations and resource-limited areas for the benefit of both humans and animals. Successful environmental detection of influenza viruses at a live bird market in a tropical climate with same-day results supports the feasibility of surveillance at human–animal interfaces with limited access to laboratories[34]. Portable and battery-driven tools such as the Bento lab (Bento Bioworks Ltd.) and the MinION (Oxford Nanopore Technologies) make genomic surveillance feasible outside traditional laboratories[35–40]. Even simple adaptations, such as using a rice cooker for agarose gel preparation, illustrate local feasibility. The entire setup fits into three suitcases, excluding the ARB ZERO 69 L fridge-freezer which can be switched for a smaller alternative, enabling transport to remote areas. Beyond technical feasibility, such field deployment demonstrates that genomic surveillance can be conducted directly near the point of sampling rather than relying on distant reference laboratories. Furthermore, in resource-limited settings, diagnostic laboratories may be constrained to testing for one or two specific viral genera due to limited financial and technical resources[41]. In this way, the PiiP assay could support situational awareness and One Health preparedness, subject to further operational validation.

Building on these results, future work should focus on expanding the PiiP panel to include additional viral genera of regional and global concern, such as those linked to hemorrhagic, neurological, or vesicular syndromes. A modular multiplex format allowing users to select primer panels relevant to local epidemiology would increase flexibility. Evaluating detection across varying viral loads in mixed samples would help characterize competition affecting low-abundance targets; this assessment was beyond the scope of the present study. Future studies could also explore the integration of host genetic markers into the workflow, enabling simultaneous identification of pathogens and hosts, to further enhance its One Health surveillance value. Additional field validation using fresh

clinical specimens and environmental samples collected under outbreak conditions will be important to assess turnaround time, usability, and robustness for early warning responses.

The PiiP assay combines degenerate panviral primers, integrated Nanopore indices, and real-time analysis to support portable screening for selected zoonotic viral groups. Evaluation in human, animal, and environmental samples, followed by field deployment using environmental samples as test-of-concept, demonstrated a route to decentralized genomic surveillance. Variable sensitivity, incomplete reference coverage, carryover, and limited influenza subtype resolution require careful interpretation and confirmatory testing. Further field deployments will determine how this approach can contribute to surveillance and outbreak investigation.

Methods

Panviral integrated indexed primer assay

Primer design and indexing

Degenerate panviral primers targeting *Alphainfluenzavirus*, *Alpha-, Beta-*, and *Gammacoronavirus* (CoVs), *Lyssavirus*, and *Orthoflavivirus* were used to generate the PiiPs. Primers targeting the *Alphainfluenzavirus* matrix gene and coronavirus ORF1ab were designed as previously described [31]. For Orthoflaviviruses, 97 complete genome sequences were downloaded from GenBank and aligned using BioEdit (v7.2.6). Consensus sequences from the alignment were used to design primers in the conserved non-structural protein 5 (NS5) region using Primer3Plus. Primers targeting the *Lyssavirus* nucleoprotein were adopted from De Benedictis *et al.* [42] (Table 1). All primers targeted the conserved genes of each viral genus to support detection of known and potentially divergent viruses. For each targeted viral genus, the forward primer was modified to integrate Oxford Nanopore native barcoding (NB) indexes, following previously published influenza sequencing workflows [21,22]. All primers were synthesized with 5’-end phosphorylation to facilitate adaptor ligation during library preparation. The complete list of PiiP sequences is provided in Supplementary Table 3.

Table 1
Unindexed panviral primer overview

Viral Genus	Primer	Unindexed Primer Sequence (5'-3')	Primer Target	Amplicon Size	Ref
Alphainfluenzavirus	Forward	GAGYCTTCTAACCGAGGTCGAAACG	Matrix protein	166bp	31
	Reverse	AGTCAGAGGTGACAGGATHGGTCT			
Alpha-, Beta-, and Gammacoronavirus	Forward	HCTTATGGGTTGGGAYTAYCC	Open reading frame 1ab	228bp	31
	Reverse	WAAGCAGTWGTDGCATCWCCD			
Orthoflavivirus	Forward	NGCNATHTGGTWYATGTGGY	Non-structural protein 5	204bp	This study
	Reverse	GTGTCCCANCCNGCNGTGTCR			
Lyssavirus	Forward	AACACYYCTACAATGGA	Nucleoprotein	603bp	42
	Reverse1	TCCAATTNGCACACATTTTGTG			
	Reverse2	TCCARTTAGCGCACATYTTATG			
	Reverse3	TCCAGTTGGCRCACATCTTRTG			

Samples included in the study

All samples used in this study were obtained from the Institut Pasteur du Cambodge (IPC) biobank and derived from ongoing surveillance activities and previously approved research projects conducted in Cambodia. Samples were stored at -80°C and thawed immediately prior to use. Sample collection, handling, and testing were performed in accordance with national regulations and institutional guidelines for human and animal research. Human clinical samples (including respiratory specimens positive for influenza A viruses or SARS-CoV-2) were collected through routine public health surveillance and response undertaken by IPC as the National Influenza Center of Cambodia, a WHO H5 Reference Laboratory, and a WHO COVID-19 Reference Laboratory. All samples were anonymized and de-identified. Animal-derived samples included post-mortem dog brain tissue collected for rabies surveillance and diagnosis, non-lethal rectal or fecal swabs from bats, poultry swabs, laboratory-reared mosquitoes, and environmental specimens. No animals were euthanized specifically for the purposes of this study. All animal sampling procedures complied with applicable animal welfare regulations. Environmental samples, including poultry drinking water, carcass wash water, cage swabs, and air samples collected in live bird markets, were obtained using non-invasive methods that did not involve human subjects or personal data. Sampling activities were conducted with appropriate local permissions and used non-invasive sampling of market environments. All laboratory work involving infectious materials was conducted in facilities with appropriate biosafety containment and operational procedures, in compliance with institutional biosafety regulations. Field deployment of portable laboratory equipment was performed following internal risk assessments and biosafety protocols to ensure safe handling of samples under field conditions.

Sample processing

Solid sample material, including feces, biopsies, and whole arthropods, was homogenized in 1x phosphate-buffered saline (PBS) using a battery-driven grinder (Sigma-Aldrich, Cat. No. Z359971) and sterile pestles (Sigma-Aldrich, Cat. No. Z359963). The homogenized material was used as input for nucleic acid extraction. Swab samples (cloacal/rectal, throat, nasopharyngeal) and air samples collected in Viral Transport Medium (VTM

composition: 2.95% Tryptose Phosphate Broth, 5.00% Gelatine, Penicillin [10,000 U/mL]–Streptomycin [10 mg/mL], Gentamycin [50 mg/mL], and 0.85% NaCl saline water, pH 7.2–7.4) were processed directly for extraction. Liquid samples, including virus culture, environmental water, and whole blood, were used directly without further preparation.

Nucleic acid extraction was performed using the QIAamp® Viral RNA Mini Kit (Qiagen, Cat. No. 52906) following the manufacturer's instructions. RT-PCR amplification was conducted on a T100 Biorad™ Thermo Cycler under the following conditions: 30 minutes at 50°C, 15 minutes at 95°C, followed by 40 cycles of 30 seconds at 94°C, 30 seconds at 52°C and 45 seconds at 72°C, with a final extension for 10 minutes at 72°C.

Amplicons were visualized on a 2% agarose gel (Invitrogen™, Cat. No. 16500100) stained with PAGE GelRed® Nucleic Acid Gel Stain (Biotium, Cat. No. NC1712531) alongside a 100 bp ladder (Invitrogen™, Cat. No. 15628019) to confirm expected amplicon sizes (Table 1; Supplementary Fig. 1).

Detection thresholds and inhibition in spiked matrices

Detection thresholds and potential inhibition in complex sample matrices were evaluated by spiking virus-negative specimens with cell culture-grown virus stocks. For *Alphainfluenzavirus* testing, chicken throat swabs in VTM and live bird market wash water were spiked with influenza A/H5N1 (A/duck/Cambodia/h2ppchba 24, 1D2T/2023). *Betacoronavirus* testing was performed by spiking homogenized bat gut tissue in PBS with SARS-CoV-2 stock (isolate 1775, Wuhan-Hu-1 strain, GISAID: EPI_ISL_956384). *Orthoflavivirus* testing used 20 homogenized *Aedes albopictus* mosquitoes in PBS spiked with dengue virus type 1 (DENV-1, strain Hawaii, 1.5 × 10^6 FFU/mL, GenBank accession KM204119.1). *Lyssavirus* testing used 150 mg of dog brain homogenized in PBS and spiked with rabies virus (RABV, Challenge Virus Standard strain CVS-11). For each viral genus, a seven-step, 10-fold dilution series was prepared. Negative controls consisted of non-spiked aliquots, while positive controls consisted of cultured isolates without homogenized material. All aliquots were extracted and processed with the PiiP assay. Amplicons were visualized on agarose gel (see Sample processing) and subsequently sequenced using Oxford Nanopore Technology (see Nanopore sequencing).

Fourplex assay configuration and co-detection

The PiiP assay was configured to run as a fourplex assay with optimized primer concentrations of 900 nM for Orthoflaviviruses and coronaviruses, 400 nM for *Lyssavirus*, and 100 nM for *Alphainfluenzavirus* (Supplementary Table 4). Assay performance was assessed using diverse viral targets, including Alphainfluenzaviruses (H1N1, H3N2, H5N1, H7N7, H9N2), Orthoflaviviruses (dengue virus serotypes 1 and 2 [DENV-1, DENV-2], Japanese encephalitis virus [JEV], Zika virus [ZIKV]), *Betacoronavirus* (SARS-CoV-2), and *Lyssavirus* (RABV). To evaluate multiplex performance, artificial viral mixtures containing representatives of each genus (H5N1, SARS-CoV-2, DENV-1, RABV) were processed with the PiiP assay to assess co-detection capability within a single reaction.

Evaluation in environmental animal and human samples

The PiiP assay was evaluated using environmental, animal, and human clinical samples of biological and epidemiological relevance. For Alphainfluenzaviruses, 10 animal and nine environmental samples from live bird markets and 11 human clinical samples were processed. For coronaviruses, 10 rectal swabs from bats and 11 clinical human samples (10 positive and one negative for SARS-CoV-2) collected in Cambodia were processed. For Lyssaviruses, 10 RABV-positive dog brain swabs and one negative macaque brain biopsy from Cambodia were tested. For Orthoflaviviruses, 11 laboratory-reared mosquitoes (*Aedes albopictus* and *Ae.* aegypti), nine of which

were infected with DENV-1, were processed. Negative controls consisted of equivalent sample types confirmed negative for the respective viral genera.

Nanopore sequencing

Library preparation

Following PCR amplification, library preparation and sequencing were performed using the Ligation Sequencing Kit (SQK-LSK114, Oxford Nanopore Technologies) with a modified protocol (Fig. 1). The forward primers, each containing a unique individual index compatible with Oxford Nanopore Native Barcodes, simplified library preparation by removing the individual barcode ligation step from the standard workflow. By omitting individual barcode ligation, dependent library preparation steps could also be omitted, including end-preparation, barcode ligation, multiple XP bead cleanups, DNA concentration measurements, and individual sample normalization. PCR products were pooled in equal volumes, and the pooled library was normalized to 30 ng before ligation with the Ligation Adaptor (LA) supplied with the Ligation Sequencing Kit using the NEBNext Quick Ligation kit following the manufacturers recommendations. The adaptor-ligated library was then purified with a single Ampure XP bead cleanup step and normalized to 50 fmol and loaded onto a R.10v flow cell for sequencing.

To reduce costs and consumable use, libraries were sequenced on washed flow cells initially utilized for routine influenza sequencing at the Institut Pasteur du Cambodge. Sequencing ran for two hours using a MinION Mk1B device connected to a Predator Triton 300 laptop. Each sequencing run included a negative control to monitor contamination and barcode spillover effects. Sequencing was performed with a minimum read length threshold of 20 bp, high-accuracy basecalling, and barcode trimming enabled.

Data analysis

Sequence data were classified and visualized in real-time using the MyTax2 analytical module (https://github.com/jhuapl-bio/mytax), which performs k-mer-based taxonomic classification using Kraken2[43] deployed within the open-source Basestack platform (v2.4.7, https://basestackwebsite.readthedocs.io/en/latest/)[26]. Viral read assignment was performed using the RefSeq k2 viral genomes database (version 20231009) available at https://genome-idx.s3.amazonaws.com/kraken/k2_viral_20231009.tar.gz and visualized as sunburst plots within MyTax2 (Supplementary Fig. 2). To account for the potential carryover associated with reused flow cells, a run-specific detection threshold was defined empirically: viral read counts had to be at least three times the corresponding count in the negative control for a sample to be classified as positive.

For selected samples, where further validation was required due to MyTax2 limitations, nanopore reads were also analyzed in Geneious Prime (version 2024.2–2025.0.3). Raw reads were quality-trimmed at both ends to a minimum quality score of 9 using BBDuk, with reads < 150 bp discarded. Reads were mapped to known reference sequences using Minimap2, and target amplicons were confirmed by alignment within the primer-binding regions. To further assess taxonomic assignment, *de novo* assembly was performed using the Geneious mapper (medium sensitivity/fast setting), and resulting contigs were identified by BLAST searches against the nr/nt database.

Portable field laboratory

Field feasibility was evaluated using portable, battery-powered equipment assembled into a laboratory for sample processing, sequencing, and real-time analysis.

Field laboratory configuration

The PiiP assay was adapted for field use by integrating spin-column extraction, PCR amplification, optional gel electrophoresis, and Nanopore sequencing with real-time viral read characterization. A portable laboratory was assembled including the Bento Lab (Bento Bioworks Ltd.), Qubit Fluorometer (Thermo Fisher Scientific), MinION Mk1D (Oxford Nanopore Technologies), EcoFlow RIVER 2 Pro Portable Power Station (EcoFlow), and a laptop for real-time sequencing (full equipment list in Supplementary Table 5). For agarose gel preparation outside conventional laboratory settings, a 0.6 L, 200W rice cooker was used. The equipment cost for the field laboratory was approximately USD 15,000 (Supplementary Table 5). To minimize contamination during field deployment, separate stocks of disposable consumables, including tubes, pipette tips, and other plastics, were maintained for pre-PCR and post-PCR activities. After completion of the workflow, nondisposable equipment and work surfaces were thoroughly decontaminated using RNAse AWAY™ Surface Decontaminant on the thermocycler and pipettes and SURFA'SAFE Premium spray on other objects and surfaces before subsequent use. Liquid waste was collected in a plastic container and dry waste was collected in labelled plastic bags and brought back to Institut Pasteur du Cambodge for decontamination and disposal.

Field deployment and sample collection

The portable laboratory was deployed outdoors in Phnom Penh, Cambodia, under ambient conditions exceeding 32°C and 60% relative humidity. Environmental samples were collected at the Orussey live bird market, including cage swabs, poultry drinking water, carcass wash water, and air samples (Thermo Scientific AerosolSense™). A previously characterized *Alphainfluenzavirus*-positive control and a negative extraction control (nuclease-free H_2O) were included. Samples were mixed 1:1 with VTM and processed as described in Sample processing, using only field laboratory equipment. Parallel testing was conducted with RT-qPCR assays for Alphainfluenzaviruses and Gammacoronaviruses (Supplementary Table 6).

Workflow execution in the field

The PiiP assay was performed in the following steps: (i) spin-column extraction with the Bento Lab centrifuge, (ii) PCR amplification with the Bento Lab thermocycler, (iii) preparation of 1% agarose gel using the rice cooker, (iv) gel electrophoresis and amplicon visualization with the Bento Lab transilluminator, (v) library preparation following the modified PiiP SOP (Fig. 1; Library preparation), and (vi) sequencing with the MinION Mk1D for a total runtime of 2 hours. Basecalling, classification, and visualization in real-time were performed on an ASUS laptop with MinKNOW (Oxford Nanopore Technologies) and Basestack platform. Cold chain maintenance of reagents was achieved using a car plug-in fridge-freezer (ARB Corporation Ltd.) and a Corning® CoolBox™ for short-term reagent storage during sample processing. All power was supplied by the Ecoflow power station.

Data availability

The sequencing data generated in this study have been deposited in the European Nucleotide Archive (ENA) at EMBL-EBI under accession number PRJEB107999 and will be made publicly available upon acceptance of the manuscript. The data are provided as FASTQ files following removal of human reads prior to submission. Primer sequences are listed in Supplementary Table 3. All additional data supporting the findings of this study are available within the Supplementary Information.

Code availability

The MyTax2 analytical module used for real-time taxonomic classification is publicly available at https://github.com/jhuapl-bio/mytax. No custom code was developed for this study beyond configuration of existing open-source tools.

Declarations

Competing interests

The authors declare no competing interests.

Author Contribution

A.S.F. contributed Conceptualization, Data curation, Formal analysis, Investigation, Methodology, Resources, Validation, Visualization, Writing – original draft, and Writing – review & editing; I.K.M. contributed Investigation, Methodology, and Writing – review & editing; B.M. contributed Methodology, Software, and Writing – review & editing; H.A. contributed Resources and Writing – review & editing; P.F.H. contributed Conceptualization, Funding acquisition, Project administration, and Writing – review & editing; R.I.H. contributed Conceptualization, Funding acquisition, Project administration, and Writing – review & editing; P.T. contributed Conceptualization, Methodology, and Writing – review & editing; C.E.L. contributed Conceptualization, Funding acquisition, Methodology, Project administration, and Writing – review & editing; E.A.K. contributed Conceptualization, Funding acquisition, Methodology, Project administration, Resources, Supervision, and Writing – review & editing.All authors reviewed and approved the manuscript.

Acknowledgement

The authors gratefully acknowledge the Royal Government of Cambodia for its continued support of infectious disease surveillance and research activities in the country. The authors thank the Ministry of Health and the Ministry of Agriculture, Forestry and Fisheries, as well as national and provincial authorities, for their collaboration, guidance, and facilitation of field and laboratory activities associated with this work. The authors also acknowledge the dedicated field teams involved in sample collection and on-site operations, whose expertise, flexibility, and commitment made the implementation of environmental, animal, and vector sampling possible under challenging field conditions. Their efforts were essential to the successful deployment of portable laboratory workflows and same-day genomic surveillance. The authors thank Dr. Sébastien Boyer and the Medical and Veterinary Entomology Unit at the Institut Pasteur du Cambodge for providing mosquito samples and for their continued collaboration and expertise in vector surveillance. The authors are also grateful to the staff of the Virology Unit, Institut Pasteur du Cambodge, for their technical assistance, logistical support, and contributions to laboratory and field activities throughout the course of this study including Dr. Janin Nouhin, Dr. Teyputita Ou, Vireak Heang, Vibol Hul, Limmey Khun, Chenthearath Rith, Sonita Kol, Kimhoung Sour, Soursdey Chanta, Sithun Noun, Saraden In, Kim Lay Chea, Reaksa Lim, and Sreymom Ken.

Data Availability

The sequencing data generated in this study have been deposited in the European Nucleotide Archive (ENA) at EMBL-EBI under accession number PRJEB107999 and will be made publicly available upon acceptance of the manuscript. The data are provided as FASTQ files following removal of human reads prior to submission. Primer sequences are listed in Supplementary Table 3. All additional data supporting the findings of this study are available within the Supplementary Information. The MyTax2 analytical module used for real-time taxonomic classification is publicly available at https://github.com/jhuapl-bio/mytax. No custom code was developed for this study beyond configuration of existing open-source tools.

References

1. Álvarez-Lerma, F. et al. Delay in diagnosis of influenza A (H1N1) pdm09 virus infection in critically ill patients and impact on clinical outcome. *Crit. Care* 20, 337 (2016).
2. Kellerborg, K., Brouwer, W. & van Baal, P. Costs and benefits of early response in the Ebola virus disease outbreak in Sierra Leone. *Cost Eff. Resour. Alloc.* 18, 13 (2020).
3. Lim, C. T. et al. Nipah viral encephalitis or Japanese encephalitis? MR findings in a new zoonotic disease. *AJNR Am. J. Neuroradiol.* 21, 455–461 (2000).
4. Zeller, M. et al. Emergence of an early SARS-CoV-2 epidemic in the United States. *Cell* 184, 4939–4952. e4915 (2021).
5. Zhang, L. L., Zhang, C. & Peng, J. P. Application of nanopore sequencing technology in the clinical diagnosis of infectious diseases. *Biomed. Environ. Sci.* 35, 381–392 (2022).
6. Allen, T. et al. Global hotspots and correlates of emerging zoonotic diseases. *Nat. Commun.* 8, 1124 (2017).
7. Jones, K. E. et al. Global trends in emerging infectious diseases. *Nature* 451, 990–993 (2008).
8. Horwood, P. F. et al. Aerosol exposure of live bird market workers to viable influenza A/H5N1 and A/H9N2 viruses, Cambodia. *Zoonoses Public Health* 70, 171–175 (2023).
9. Delaune, D. et al. A novel SARS-CoV-2 related coronavirus in bats from Cambodia. *Nat. Commun.* 12, 6563 (2021).
10. Auerswald, H. et al. Bayesian modeling of post-vaccination serological data suggests that yearly vaccination of dog aged < 2 years old is efficient to stop rabies circulation in Cambodia. *PLoS Negl. Trop. Dis.* 18, e0012089 (2024).
11. Maquart, P., Fontenille, D. & Boyer, S. Recent and massive invasion of aedes (Stegomyia) albopictus (Skuse, 1894) in Phnom Penh, Cambodia. *Parasit. Vectors* 14, 1–3 (2021).
12. Simner, P. J., Miller, S. & Carroll, K. C. Understanding the promises and hurdles of metagenomic next-generation sequencing as a diagnostic tool for infectious diseases. *Clin. Infect. Dis.* 66, 778–788 (2018).
13. Hsu, W.-Y. et al. Performance of a hybrid capture-based target enrichment next-generation sequencing for the identification of respiratory pathogens and resistance-associated genes in patients with severe pneumonia. *Microbiol. Spectr.* 13, e02130-02124 (2025).
14. Gaston, D. C. et al. Evaluation of metagenomic and targeted next-generation sequencing workflows for detection of respiratory pathogens from bronchoalveolar lavage fluid specimens. *J. Clin. Microbiol.* 60, e00526-00522 (2022).
15. Holbrook, M. G. et al. Updated and validated pan-coronavirus PCR assay to detect all coronavirus genera. *Viruses* 13, 599 (2021).

16. Wang, X. et al. A pan-coronavirus RT-PCR assay for rapid viral screening of animal, human, and environmental specimens. *One Health* 13, 100274 (2021).
17. Chen, N. F. et al. Development of an amplicon-based sequencing approach in response to the global emergence of mpox. *PLoS Biol.* 21, e3002151 (2023).
18. Reteng, P. et al. A targeted approach with nanopore sequencing for the universal detection and identification of flaviviruses. *Sci. Rep.* 11, 19031 (2021).
19. Schlaberg, R. et al. Viral pathogen detection by metagenomics and pan-viral group polymerase chain reaction in children with pneumonia lacking identifiable etiology. *J. Infect. Dis.* 215, 1407–1415 (2017).
20. WHO Pathogens prioritization: a scientific framework for epidemic and pandemic research preparedness. World Health Organization, Geneva (2024).
21. Edwards, K. M. et al. Detection of Clade 2.3.4.4b Avian Influenza A(H5N8) Virus in Cambodia, 2021. *Emerg. Infect. Dis.* 29, 170–174 (2023). https://doi.org/10.3201/eid2901.220934.
22. Thielen, P. Influenza whole genome sequencing with integrated indexing on Oxford Nanopore platforms. protocols.io https://doi.org/10.17504/protocols.io.kxygxm7yzl8j/v1 (2022).
23. Kalantar, K. L. et al. IDseq—An open source cloud-based pipeline and analysis service for metagenomic pathogen detection and monitoring. *GigaScience* 9, giaa111 (2020).
24. Simmonds, S. E. et al. CZ ID: a cloud-based, no-code platform enabling advanced long read metagenomic analysis. *bioRxiv* 2024.02.29.579666 (2024).
25. The Galaxy Community The Galaxy platform for accessible, reproducible, and collaborative data analyses: 2024 update. *Nucleic Acids Res.* 52, W83-W94 (2024).
26. Merritt, B. Basestack. Version 2.4.7. Released 15 December 2020. https://github.com/jhuapl-bio/Basestack (2020).
27. Sievers, B. L. et al. “Smart markets”: harnessing the potential of new technologies for endemic and emerging infectious disease surveillance in traditional food markets. *J. Virol.* 98, e01683-01623 (2024).
28. Li, W. et al. Bats are natural reservoirs of SARS-like coronaviruses. *Science* 310, 676–679 (2005).
29. Ruiz-Aravena, M. et al. Ecology, evolution and spillover of coronaviruses from bats. *Nat. Rev. Microbiol.* 20, 299–314 (2022).
30. Possas, C. et al. Zika puzzle in Brazil: peculiar conditions of viral introduction and dissemination-a review. *Mem. Inst. Oswaldo Cruz* 112, 319–327 (2017).
31. Meki, I. K. et al. Novel multiplex family-wide PCR and Nanopore sequencing of amplicons (FP-NSA) approach for surveillance of influenza-and coronaviruses in humans and animals. *Genome Med.* 17, 123 (2025).
32. Oxford Nanopore Technologies. Flow Cell Wash Kit - EXP-WSH004, https://store.nanoporetech.com/flow-cell-wash.html.
33. Sanderson, N. D. et al. Real-time analysis of nanopore-based metagenomic sequencing from infected orthopaedic devices. *BMC Genomics* 19, 714 (2018).
34. Gavina, K., Franco, L. C., Khan, H., Lavik, J.-P. & Relich, R. F. Molecular point-of-care devices for the diagnosis of infectious diseases in resource-limited settings–A review of the current landscape, technical challenges, and clinical impact. *J. Clin. Virol.* 169, 105613 (2023).
35. Faria, N. R. et al. Mobile real-time surveillance of Zika virus in Brazil. *Genome Med.* 8, 97 (2016).

36. Fomsgaard, A. S. et al. Unbiased virus detection in a Danish zoo using a portable metagenomic sequencing system. *Viruses* 15, 1399 (2023).
37. Hirabayashi, A. et al. On-site genomic epidemiological analysis of antimicrobial-resistant bacteria in Cambodia with portable laboratory equipment. *Front. Microbiol.* 12, 675463 (2021).
38. Kitamura, K., Ueno, M. K. & Yoshida, H. Rapid and sensitive on-site detection of SARS-CoV-2 RNA from environmental surfaces using portable laboratory devices. *Microbiol. Spectr.* 11, e00456-00423 (2023).
39. Marin, C. et al. Rapid oxford nanopore technologies MinION sequencing workflow for Campylobacter jejuni identification in broilers on site—a proof-of-concept study. *Animals* 12, 2065 (2022).
40. Quick, J. et al. Real-time, portable genome sequencing for Ebola surveillance. *Nature* 530, 228–232 (2016).
41. Stevenson, M. & Halpin, K. Emerging and endemic zoonotic diseases: surveillance and diagnostics. *Rev. Sci. Tech.* 40, 119–129 (2021).
42. De Benedictis, P. et al. Lyssavirus detection and typing using pyrosequencing. *J. Clin. Microbiol.* 49, 1932–1938 (2011).
43. Wood, D. E., Lu, J. & Langmead, B. Improved metagenomic analysis with Kraken 2. *Genome Biol.* 20, 257 (2019).

Figures

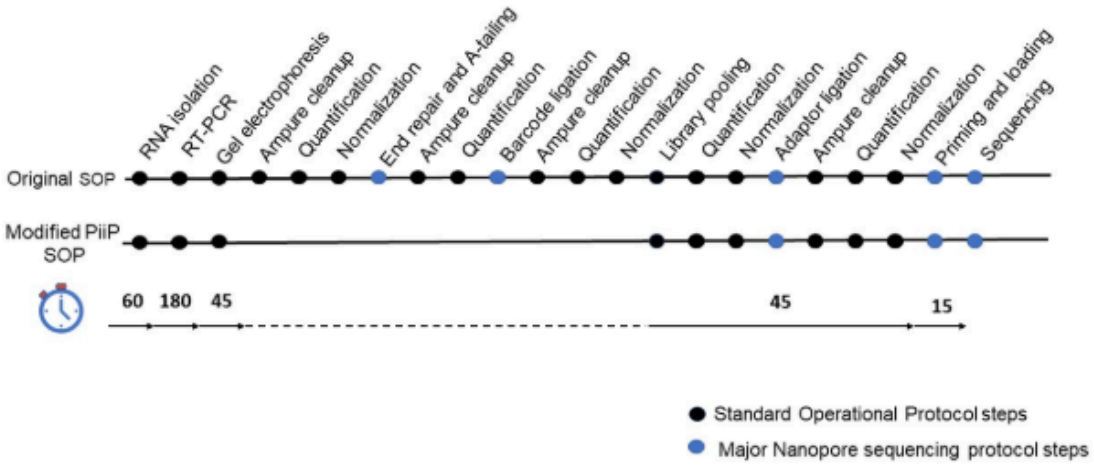


Figure 1

Comparison of conventional and PiiP workflows. The conventional standard operating procedure (SOP) uses unindexed panviral primers with the Oxford Nanopore Ligation Sequencing Kit (SQK-LSK114), whereas the modified PiiP SOP uses indexed panviral primers. Black and blue dots indicate steps included or omitted in each workflow. After gel electrophoresis, the modified PiiP SOP omits 10 steps from the conventional SOP. Equal volumes of each RT-PCR product are pooled, quantified and normalized for adaptor ligation, allowing extraction to the start of sequencing to be completed in under 7 hours.

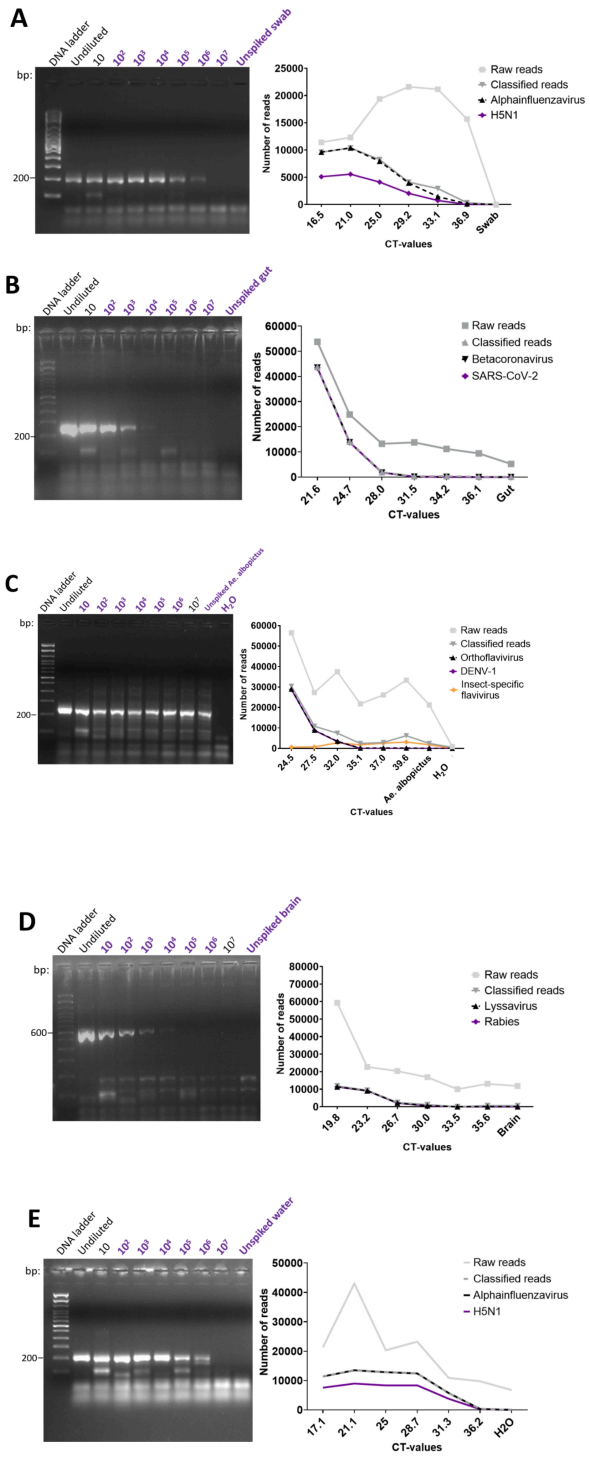


Figure 2

Detection thresholds of the PiiP assay in spiked host-derived and environmental matrices. Gel electrophoresis images and sequencing results from spiking experiments are shown with the Cq detection thresholds for genus (Cq_g) and subtype/species (Cq_s): a, *influenza* A/H5N1 in chicken throat swabs (Cq_g 36.9; Cq_s ≤33.1); b, SARS-CoV-2 in homogenized bat gut (Cq_g 34.2; Cq_s 34.2); c, DENV-1 in homogenized *Aedes albopictus* (Cq_g 39.6; Cqs ≤32.0); d, RABV in homogenized dog brain (Cq_g ≤30.0; Cq_s ≤30.0); and e, influenza A/H5N1 in poultry carcass wash water

from a live bird market (Cq_g 36.2; Cq_s 36.2). Dilutions subjected to sequencing are highlighted in bold purple text in the corresponding gel images. Line plots were generated in GraphPad Prism 10 (version 10.3.0).

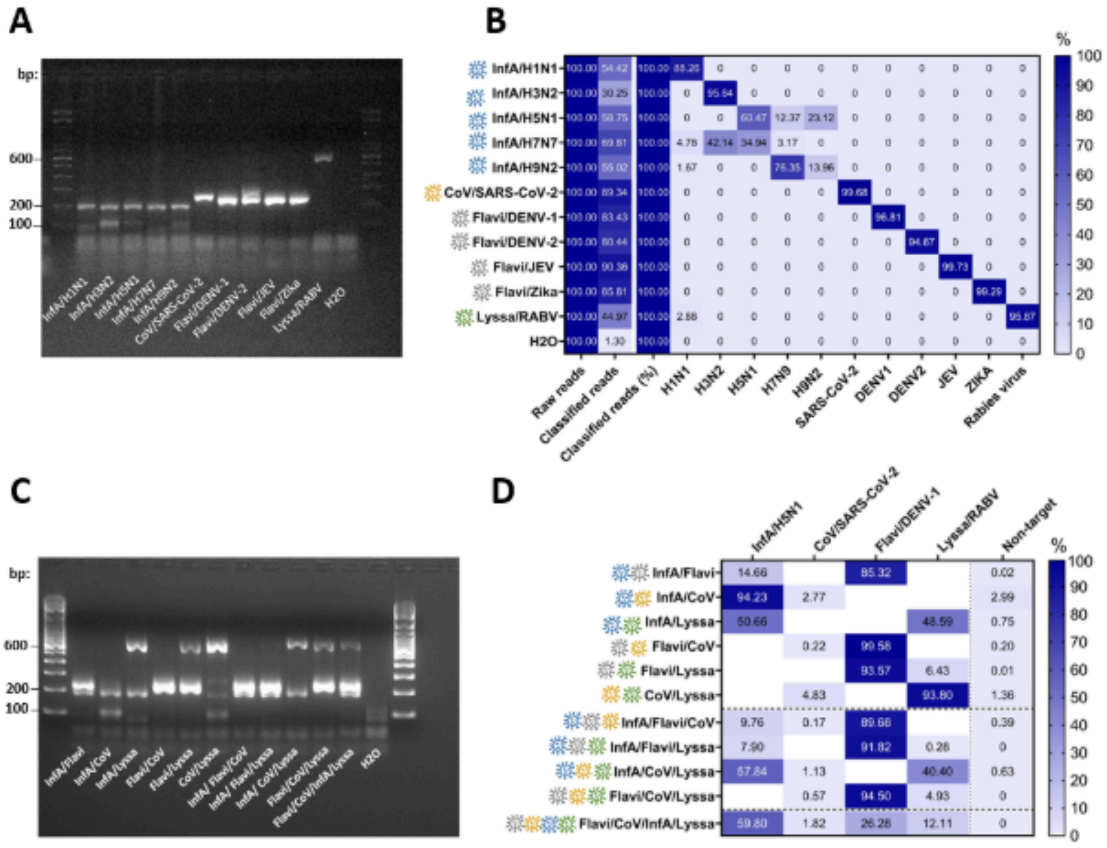


Figure 3

Fourplex genotyping and co-detection performance of the PiiP assay. a, Gel electrophoresis of PCR products from the fourplex genotyping assay targeting H5N1, SARS-CoV-2, DENV-1 and RABV. b, Sequencing output analysed using MyTax2 within Basestack, showing read assignments by subtype. Raw reads were normalized to 100%; columns show the percentage of classified reads assigned to each subtype, and rows represent individual tested samples. The colour gradient indicates percentage values. c, Gel electrophoresis of PCR products from artificial co-infection mixtures containing two, three or four viral targets. d, Distribution of classified sequencing reads across viral targets in artificial co-infection mixtures, analysed in Geneious Prime. Columns show the percentage of reads assigned to each virus, and rows represent individual tested mixtures. The colour gradient indicates percentage values. Heatmaps were generated in GraphPad Prism 10 (version 10.3.0).

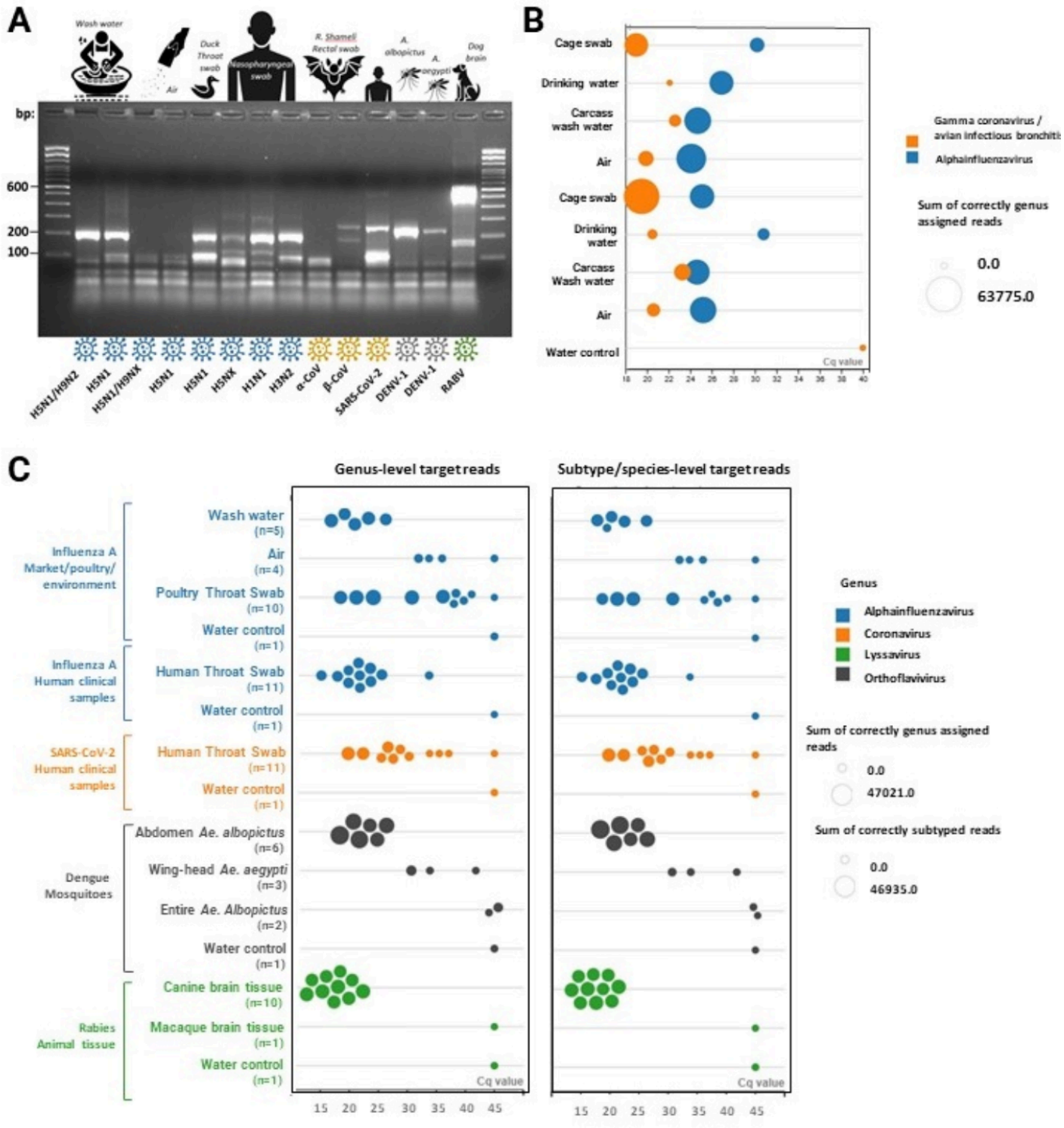


Figure 4

Detection and subtyping performance of the PiiP assay across sample matrices and virus groups. Panels a and c show laboratory evaluation; panel b shows field deployment at a Cambodian live bird market. a, Representative PiiP assay amplicons generated from environmental, animal, vector and human clinical samples. b, Environmental samples collected and processed on site as a proof of concept using the field-deployable laboratory (Supplementary Data 1, worksheet Table S4-E). Each bubble represents one sample, and bubble size indicates the number of correctly assigned reads. c, Relationship between RT-qPCR Cq value and sequencing read recovery.

Each bubble represents one sample (Supplementary Data 1, worksheet Table S4-D). Bubble size indicates the number of correctly assigned reads at genus level (left) or species/subtype level (right). Negative samples, including water controls, are displayed at Cq 45. Bat alphacoronavirus and betacoronavirus samples that were not tested by RT-qPCR are excluded.

Supplementary Files

This is a list of supplementary files associated with this preprint. Click to download.

- SupplementaryData1.xlsx
- SupplementaryInformation.pdf